STRONGLY ROTATING ST P-^{11}B FUSION PLASMAS

A data-based model to raise confinement and fusion reaction rate is proposed.

Y.-K.M. PENG, Y. SHI, B. LIU, A. ISHIDA, W. LIU, T. SUN, D. GUO, Z. LI, D. LUO, X. XIAO, H. HUANG, G. ZHAO, D. YANG, J. DONG, M. LIU and the ENN Fusion Team.
Hebei Key Laboratory of Compact Fusion; ENN Science and Technology Development Co., Langfang, China
Email: pengyuankai@enn.cn

A Spherical Torus (ST) plasma model is proposed and investigated to meet the challenges of reaching several times higher energy confinement times than the ITER H-mode [1] and over 100 keV in ion temperature at densities over $10^{20}/m^3$ required by a p-^{11}B fusion plasma [2,3]. The model is characterized by strong toroidal rotation, flow-shear, and low-percentage thermalizing supra-thermal plasma components co-existing with the main thermalized plasma. Such plasma features can substantially improve confinement and fusion reaction rates, as seen in JET [4] and LHD [5] experiments, for plasmas below fusion burn conditions. NSTX [6], MAST [7], and Globus-M2 [8] have revealed the advantages of the ST: high toroidal beta β_T, sub-Alfven-velocity rotation, near-neoclassical level ion energy transport, and confinement scaling that leverages the toroidal field B_T and major radius R strongly. Reaching central ion temperatures of 10^8 °K in ST-40 [9] confirmed the high potential of compact strongly rotating ST p-^{11}B fusion plasmas.

ST plasma models showing some of these features have been introduced on EXL-50 [10,11] and are extended to recent data on EXL-50U with I_p up to 500 kA [12]. It is confirmed that, to reproduce all available experimental data to within a few %, the plasma equilibrium must contain thermalized proton, boron, and electron components in addition to a supra-thermal relativistic electron component that extends beyond the last closed flux surface (LCFS). As shown in Fig. 1 for peak T_i ~ 1.7 keV and n_e ~ 1.1 $10^{20}/m^3$, charge neutrality enforces a positively charged thermalized plasma within the LCFS relative to the metallic wall. Toroidal plasma rotation with shear results, presuming strong auxiliary RF and neutral beam injection heating. Co-existing supra-thermal relativistic electrons extend substantially beyond the LCFS and carry over 50% of the toroidal plasma current I_p.

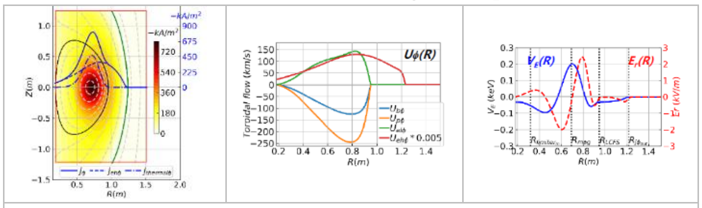

Fig. 1, A rotating plasma equilibrium projected for EXL-50U composed of thermal proton, boron, and thermal and relativistic electrons, featuring ~140 km/s rotation and ~0.2 keV potential.

Extensions to an ST p-^{11}B plasma nearing the fusion burn condition are carried out [13], based on the preceding analysis. Key parameters (in units of m, MA, T, $10^{20}/m^3$, keV) include R = 1.4, a = 0.74, I_p = 13.6, B_T = 3.5, β_T = 0.27, β_p = 1.4, β_N = 5.1, k = 2.6, δ = 0.24, q_0 = 1.5, q_{LCFS} = 5.3, l_i = 0.23, n_{e0} = 1.04, n_{p0} = 0.34, n_{B0} = 0.14, n_{ph0} = 0.004, n_{Bh0} = 0.0018, n_{eh0} = 0.036, T_{p0} = T_{B0} = 130, T_{e0} = 29, T_{ph0} = T_{Bh0} = 620, T_{eh0} = 2050. This plasma composition takes advantage of the sharp peak at 160 keV and the broad peak at ~600 keV of the p-^{11}B reaction cross section [14]. Fig. 2 shows some of the plasma profiles in the poloidal cross-section. The supra-thermal components carry substantial current, pressure, and rotation beyond the LCFS, while the thermalized plasma current remains within the LCFS. The positive potential of up to 10 kV relative to the wall bounding the plasma helps expel cold ions escaping the LCFS. The plasma forms a magnetic well and hill combination in the outboard region of the plasma, suppressing ion micro-turbulence and causing "orbit squeezing" [15] and low aspect ratio axisymmetric omnigeneity [16,17] to reduce the neoclassical ion transport, leading to τ_{Ei} ~ T_i^2.

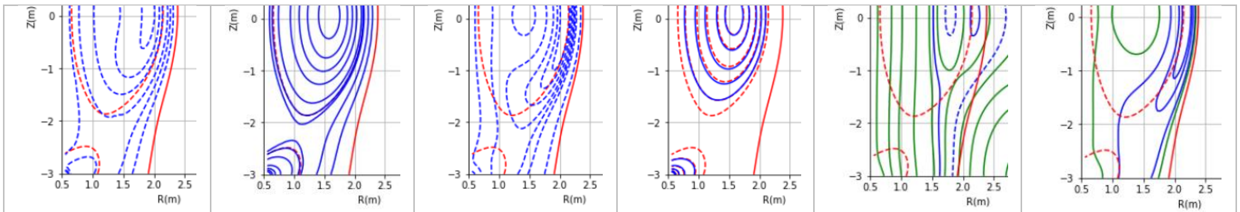

Fig. 2, Toroidal current density (-0.1~-4.0MA/m^2)	*Plasma pressure (0.01~2.5MPa)*	*Supra-thermal electron current density (-0.01~-1.45MA/m^2)*	*Electrostatic potential (1.8~11.5kV)*	*Magnetic well (2.82T) and hill (3.14T) in the omnigenous region*	*Velocity difference of supra-thermal proton and thermal boron (0.6~1.75Mm/s)*

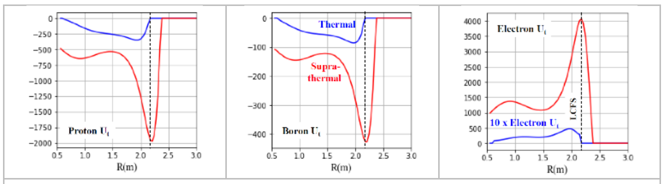

Fig. 3, Proton, boron and electron thermal (blue) and supra-thermal (red) toroidal rotation velocities

The plasma rotation profiles on the mid-plane (see, Fig. 3) show that the thermal plasma rotation and its shear sit in the region of the magnetic well. The supra-thermal proton rotation peaks near the LCFS with velocities up to 1900 km/s over the thermal boron, increasing the plasma fusion reaction rate. The inter-mixing of these components in space introduces a physics regime where microturbulence and transport properties can be modified from the standard tokamak physics regime.

The orbit confinement of the supra-thermal components will limit their maximum energies in the pitch-angle-energy space [18]. These features as modelled for the EXL-50U plasma and extended to near-burn ST p-^{11}B fusion plasmas can affect the ST properties and the p-^{11}B fusion reaction rates. Unexplored new plasma features of high importance to ST p-^{11}B fusion power will be elucidated.

ACKNOWLEDGEMENTS

Helpful discussion Drs. Liang Yunfeng, Xie Huasheng, and Yang Yuanming are gratefully acknowledged.

REFERENCES

[1] ITER Physics Expert Groups on Confinement and Transport and Confinement Modelling and Database, ITER Physics Basis Editors and ITER EDA 1999, Nucl. Fusion **39** (1999) 2175-2249.

[2] LIU, M. et al., ENN's roadmap for proton-boron fusion based on spherical torus, Phys. Plasmas **31** (2024) 062507 (14pp)

[3] PUTVINSKI, S. et al., Fusion reactivity of the pB11 plasma revisited, Nuclear Fusion **59** (2019) 076018 (9pp).

[4] KIROV, K.K. et al., Impact of interaction between RF waves and NBI ions on the fusion performance in the JET DTE2 campaign, Nucl. Fusion **64** (2024) 016026 (19 pp).

[5] MUTOH, T. et al., Steady state operation and high energy particle production of MeV energy in the Large Helical Device, Nucl. Fusion **47** (2007) 1250-1257.

[6] SABBAGH, S.A., Resistive wall stabilized plasmas in rotating high beta NSTX plasmas, Nucl. Fusion **46** (2006) 435-644.

[7] AKERS, R.J., et al., Transport and confinement in the Mega-Ampere Spherical Tokamak (MAST) plasma, Plasma Phys. Control. Fusion **45** (2003) A175-A204.

[8] KURSKIEV, G.S., et al., Tenfold increase in the fusion triple product caused by doubling of toroidal magnetic field in the spherical tokamak Globus-M2, Nucl. Fusion **61** (2021) 064001 (8pp).

[9] MACNAMARA, S.A.M. et al., Overview of recent results from the ST40 compact high-field spherical tokamak, Nucl. Fusion **64** (2024) 112020 (14pp).

[10] ISHIDA, A., et al., Four-fluid axisymmetric plasma equilibrium model including relativistic electrons and computational method and results, Phys. Plasmas **28** (2021) 032503 (16pp).

[11] MAEKAWA, T., et al., Particle orbit description of cyclotron-driven current-carrying energetic electrons in the EXL-50 spherical torus, Nucl. Fusion **63** (2023) 076014 (20pp).

[12] SHI, Y., et al., Overview of EXL-50U Experiments: Addressing Key Physics Issues for Future Spherical Tokamak p-11B Reactors, this conference.

[13] ISHIDA, A., et al., manuscript in preparation.

[14] GESER, F.A., VALENTE, M., A theoretical model for the cross section of the proton-boron fusion nuclear, Radiat. Phys. Chem. **167** (2020) 108224 (6pp).

[15] SHAING, K.C. et al., Improved neoclassical confinement and turbulence suppression in a magnetic well in tokamak reactor, Nucl. Fusion **61** (2021) 096031 (7pp).

[16] TESSAROTTO, M. et al., Omnigenous transport barriers in MHD equilibria, Phys. Letters A **222** (1996) 101-106.

[17] DUDT, D.W., et al., Magnetic fields with general omnigeneity, J. Plasma Phys **90** (2024) 905900120 (14pp).

[18] SUN, T., et al., manuscript in preparation.